Functional trait variation related to gap dynamics in tropical moist forests: a vegetation modelling perspective

Functional trait variation related to gap dynamics in tropical moist forests: a vegetation modelling perspective

Henrique Fürstenau Togashi[a,b,*], Owen K. Atkin[c,d], Keith J. Bloomfield[c], Matt Bradford[e], Kunfang Cao[f], Ning Dong[a,b,g], Bradley J. Evans[a,b], Zexin Fan[h], Sandy P. Harrison[a,g], Zhu Hua[h], Michael J. Liddell[i], Jon Lloyd[i,j], Jian Ni[k,l], Han Wang[a,m], Lasantha K. Weerasinghe[c,n], Iain Colin Prentice[a,j,m,o]

[a]Department of Biological Sciences, Macquarie University, North Ryde, NSW 2109, Australia

[b]The Ecosystem Modelling and Scaling Infrastructure Facility (eMAST), Faculty of Agriculture and Environment, Department of Environmental Sciences, The University of Sydney, NSW 2006, Australia

[c]Division of Plant Sciences, Research School of Biology, Australian National University, Canberra, ACT 2601, Australia

[d]ARC Centre of Excellence in Plant Energy Biology, Research School of Biology, Australian National University, Canberra, ACT 2601, Australia

[e]Commonwealth Science and Industrial Research Organization (CSIRO), Tropical Forest Research Centre, Atherton, Queensland 4883, Australia

[f]State Key Laboratory of Conservation and Utilization of Subtropical Agro-bioresources, College of Forestry, Guangxi University, Daxuedonglu 100, Nanning 530005, Guangxi, China

[g]School of Archaeology, Geography and Environmental Sciences, University of Reading, Whiteknights, Reading RG6 6AB, UK

[h]Key Laboratory of Tropical Forest Ecology, Xishuangbanna Tropical Botanical Garden, Chinese Academy of Sciences, Menglun, Mengla, Yunnan 666303, China

[i]Centre for Tropical Environmental and Sustainability Science (TESS) and College of Science, Technology and Engineering, James Cook University, Cairns, Queensland 4878, Australia

[j]Department of Life Sciences, Imperial College London, Silwood Park Campus, Buckhurst Road, Ascot SL5 7PY, UK

[k]State Key Laboratory of Environmental Geochemsitry, 99 Lincheng West Road, Guanshanhu, Guiyang, Guizhou 550081, China

[l]College of Chemistry and Life Sciences, Zhejiang Normal University, Yingbin Avenue 688, Jinhua 321004, Zhejiang, China
[m]Department of Earth System Science, Tsinghua University, Beijing 100084, China
[n]Faculty of Agriculture, University of Peradeniya, Peradeniya 20400, Sri Lanka
[o]State Key Laboratory of Soil Erosion and Dryland Farming on the Loess Plateau, College of Forestry, Northwest Agriculture & Forestry University, Yangling 712100, China

[*]Corresponding author (henriquetogashi@gmail.com)

ABSTRACT

The conventional representation of Plant Functional Types (PFTs) in Dynamic Global Vegetation Models (DGVMs) is increasingly recognized as simplistic and lacking in predictive power. Key ecophysiological traits, including photosynthetic parameters, are typically assigned single values for each PFT while the substantial trait variation within PFTs is neglected. This includes continuous variation in response to environmental factors, and differences linked to spatial and temporal niche differentiation within communities. A much stronger empirical basis is required for the treatment of continuous plant functional trait variation in DGVMs. We analyse 431 sets of measurements of leaf and plant traits, including photosynthetic measurements, on evergreen angiosperm trees in tropical moist forests of Australia and China. Confining attention to tropical moist forests, our analysis identifies trait differences that are linked to vegetation dynamic roles. Coordination theory predicts that Rubisco- and electron-transport limited rates of photosynthesis are co-limiting under field conditions. The least-cost hypothesis predicts that air-to-leaf CO_2 drawdown minimizes the combined costs per unit carbon assimilation of maintaining carboxylation and transpiration capacities. Aspects of these predictions are supported for within-community trait variation linked to canopy position, just as they are for variation along spatial environmental gradients. Trait differences among plant species occupying different structural and temporal niches may provide a basis for the ecophysiological representation of vegetation dynamics in next-generation DGVMs.

Keywords: plant traits, photosynthesis, vegetation dynamics, tropical forests, DGVMs

Introduction

The development of Dynamic Global Vegetation Models (DGVMs) from the earliest stages has emphasized the role of the distribution of different types of plants and vegetation in predicting the exchanges of carbon between the atmosphere and the land biota (Prentice et al., 2007; Prentice and Cowling, 2013). Plant Functional Type (PFT) classifications can be traced back to the Raunkiær's (1934) 'life form' classification, based on plant traits that ensure persistence through seasons unfavourable for growth (Harrison et al., 2010). After several decades during which plant functional geography was neglected, new PFT classifications appeared during the 1980s (Box, 1981; Woodward, 1987) with a view to the development of DGVMs – which began in earnest during the late 1980s. The PFT concept has received significant attention since then (Prentice et al., 1992; Díaz and Cabido, 1997; Lavorel and Garnier, 2002; Wright et al., 2004; Prentice et al., 2007; Harrison et al., 2010; Fyllas et al., 2012). It has become widely accepted that PFT classifications for modelling purposes ideally should reflect aspects of trait diversity that can predict plant responses to the physical environment.

PFTs adopted in DGVMs today are commonly defined in terms of up to five qualitative traits: (a) life form, (b) leaf type, (c) phenological type, (d) photosynthetic pathway and (e) climatic range defined in terms of broad climatic classes such as 'boreal' and 'tropical'. This conventional approach to PFT classification has manifold limitations (Prentice and Cowling, 2013). For example, life-forms are often incompletely defined in functional terms. Informal and potentially ambiguous terms such as 'shrub' have been used in place of Raunkiær's explicit functional categories. Leaf-type definitions usually ignore the huge variations in leaf size and shape among 'broad-leaved' plants. Even the distinction between broad and needle-leaved trees is often effectively an imperfect surrogate for the important distinction in hydraulic architecture between angiosperms and gymnosperms – the latter, in fact, including many species with broad leaves. Thermal climate categories may make sense if they are recognized as a surrogate for different cold-tolerance mechanisms in phanerophytes (Prentice et al., 1992). Harrison et al. (2010) provided a more recent compilation of experimental data on cold tolerance. However, such categories are often used without clear definitions. They may stand in for a continuum of physiological differences between plants adapted or acclimated to different seasonal

temperature regimes, rather than representing qualitative differences among distinct types of plant. Moreover, thermal climate categories may artificially restrict modelled PFT distributions within confined areas even if the absence of a given PFT from a wider area could be due to competitive exclusion by other types. Ideally, shifts of dominance in models should not be imposed in this way, but should emerge naturally through competitive advantage (Fisher et al., 2015).

A distinct aspect of plant functional classification pertains to species' 'roles' in vegetation dynamics. Classifications of tree species according to shade tolerance (Whitmore, 1982), growth characteristics: maximum height and growth rate (Shugart, 1984; Swaine and Whitmore, 1988) and successional stage (pioneer *versus* climax) Swaine and Whitmore (1988) have been a mainstay of regionally specific 'gap models' designed to predict forest dynamics under constant or changing environmental conditions (Botkin et al., 1972; Shugart, 1984; Denslow, 1987; Prentice and Leemans, 1990; Prentice et al., 1993; Turner, 2001) but are not treated by most DGVMs. Exceptions are those models with individual-based dynamical cores, such as LPJ-GUESS (Smith et al., 2001), Hybrid (Friend et al., 1993), ED (Moorcroft et al., 2001; Medvigy et al., 2009), aDGVM2 (Langan et al., 2017), and models that make use of the Perfect Plasticity Approximation (PPA). PPA is a mathematical approach designed to represent the essentials of forest dynamics without simulating individual trees explicitly (Purves et al., 2008; Fyllas et al., 2014; Fisher et al., 2015).

A general critique of the use of PFTs for modelling purposes has emerged with the development of new dynamic vegetation models based on continuous trait variation (Pavlick et al., 2013; Scheiter et al., 2013; Verheijen et al., 2013; Fyllas et al., 2014; van Bodegom et al., 2014; Sakschewski et al., 2015), raising a question as to whether distinct PFTs are necessary for modelling vegetation. In our view there is a clear-cut case for retaining the well-understood distinctions among photosynthetic pathways, and there may also be good reasons also to retain life-form distinctions – at least at the highest level of Raunkiær's classification. However, most quantitative traits show continuous adaptive variation along environmental gradients (Meng et al., 2015), indicating that the conventional approach of assigning fixed values of leaf-level traits such as carboxylation capacity (V_{cmax}) and nitrogen content per unit leaf area (N_{area}) to PFTs does not adequately describe the plasticity of such traits within species (phenotypic plasticity). Even biophysical traits such as leaf mass per area

(LMA) and leaf dry-matter content, which are typically less plastic than metabolic traits (Meng et al., 2015; Dong et al., 2017), show systematic, quantitative variations along environmental gradients, partly as a consequence of species turnover within PFTs and thus not necessarily the replacement of one PFT by another. Faced with continuous trait variation (due to species or genotypic turnover and/or phenotypic plasticity), models can either treat it as continuous – as the LPJ DGVM (Sitch et al., 2003) does for photosynthetic traits, following the approach developed by Haxeltine and Prentice (1996) – or subdivide the continuum into arbitrary sections. However, problems such as unrealistically abrupt modelled vegetation transitions can arise if the subdivision of the continuum is too coarse, suggesting that a continuous representation will be more useful.

This paper describes an empirical analysis that is oriented towards the improvement of DGVMs. Our primary focus is on the largely neglected 'dynamical' aspect of PFT classification. We adopt the fourfold scheme introduced by Shugart (1984) as an initial scheme to classify species' dynamic roles. We recognize that this classification represents a subdivision of two orthogonal continua of variation: shade tolerance (requiring, *versus* not requiring, a gap for regeneration) and size at maturity (producing, *versus* not producing, a gap upon mortality). We focus on functional trait variations within tropical moist forests, which harbour enormous tree species diversity and contain species that exhibit all combinations of these traits (Turner, 2001). We build on a previous analysis by Fyllas et al. (2012), who showed that quantitative traits including foliar $\delta^{13}C$ discrimination, LMA and nutrients including N and P could be used to discriminate PFTs with distinct dynamic characteristics in Amazonian rain forests. Our analysis focuses on east Asian (SW China) and northern Australian tropical rain forests, and extends the approach of Fyllas et al. (2012) to include field photosynthetic measurements.

Theory and Principles

Recent empirical analyses aiming to inform the development of 'next-generation' DGVMs have focused on the predictability of key quantitative traits as a function of environmental variation (Yang et al., 2018). The 'least-cost' (Prentice et al., 2014) and 'coordination' (Maire et al., 2012) hypotheses together suggest a degree of predictability for the air-to-leaf CO_2 drawdown (χ, the ratio of leaf-internal to

ambient CO_2) (Prentice et al., 2014; Wang et al., 2017), V_{cmax} and the electron-transport capacity J_{max} (Togashi et al., 2017), and N_{area} (Dong et al., 2017) across environments and clades. Both hypotheses have a much longer pedigree than indicated by the recent references cited here, but systematic testing of these hypotheses has only been undertaken quite recently.

The least-cost hypothesis proposes that at the leaf level, plants should respond to differences in the relative costs (per unit of assimilation achieved) of maintaining the biochemical capacity for photosynthesis *versus* the structural capacity for transpiration by making an optimal investment 'decision' that minimizes the total carbon cost of maintaining both essential functions. This hypothesis can be shown to lead to an optimum value of χ that depends predictably on temperature, vapour pressure deficit and atmospheric pressure (Prentice et al., 2014; Wang et al., 2017). The mathematical expression of this optimum value includes a parameter that is influenced by low plant-available moisture, and therefore by soil moisture and rooting characteristics (Zhou et al., 2013). This optimum has the same mathematical form as that predicted approximately by the Cowan-Farquhar optimality criterion for electron-transport limited photosynthesis. This form is known to provide good predictions of stomatal behaviour under a range of conditions (Medlyn et al., 2011; Lin et al., 2015; Dewar et al., 2018). The least-cost hypothesis however is more explicit than the Cowan-Farquhar criterion in that it 'unpacks' water transport and biochemical costs, and assigns to each of them an explicit ecophysiological meaning.

The coordination hypothesis indicates that under typical daytime conditions, the Rubisco-limited and electron transport-limited rates of photosynthesis should be approximately equal (Chen et al., 1993; Haxeltine and Prentice, 1996; Maire et al., 2012). This represents the optimal disposition of resources between light capture and carbon fixation. It leads to the prediction that the outer-canopy V_{cmax} measured at the prevailing growth temperature should be determined by χ (higher values of one quantity are consistent with lower values of the other), temperature (higher V_{cmax} is required to achieve a given assimilation rate at higher temperatures), and incident photosynthetically active radiation (PAR) (productive investment in V_{cmax} is directly proportional to the available PAR) (Dong et al., 2017). N_{area} is generally found to be roughly linearly related to Rubisco content, and thus to V_{cmax} at standard temperature. However, leaf N also has structural and defensive components that are roughly proportional to LMA and represent a largely independent source of variation in N_{area}

(Dong et al., 2017). So far, these predictions have been supported for seasonal variations within individual plants (Togashi et al., 2017), and for spatial variations along environmental gradients (Prentice et al., 2014; Dong et al., 2017). Here we extend their application to biotically conditioned, microenvironmental variation within forest environments. The framework provided by the least-cost and coordination hypotheses suggest moreover that shade tolerance, and stem properties such as height and wood density, should also be related to leaf metabolic and structural traits, as proposed by Whitehead et al. (1984) and many later commentators.

The least-cost and coordination hypotheses are optimality concepts, whose rationale depends on the heuristic principle that natural selection is expected to have eliminated all trait combinations that fall short of optimality according to some specified criterion. Another optimality concept lies behind the Leaf Economics Spectrum, LES (Wright et al., 2004). Fundamentally, the LES represents a universal negative correlation between LMA and leaf life-span (Lloyd et al., 2013), which can be considered to arise from a trade-off because (a) carbon available for investment in leaves is limited and (b) long-lived leaves need to be thicker and/or tougher than short-lived leaves in order to avoid high risks of predation by herbivores and other kinds of mechanical damage. Thus leaves can be short-lived and flimsy or long-lived and thick and/or tough, or somewhere in between. In contrast, short-lived leaves with high LMA would be uneconomic, while long-lived leaves with low LMA would be unviable.

In this study we consider four groups of leaf and stem traits. The first group consists of leaf metabolic traits: V_{cmax}, J_{max} and leaf dark respiration (R_{dark}), which has been found to correlate with V_{cmax} (Atkin et al., 2000; Weerasinghe et al., 2014). The second group contains the leaf structural/chemical traits N_{area}, P_{area} and LMA. As previously noted, N_{area} has a metabolic component as well as a structural component, and the same may be true for P_{area} (Evans, 1989; Reich et al., 1997; Fyllas et al., 2009). But increasing evidence points to the dominance of the structural component when large sets of species are considered (Dong et al., 2017; Yang et al., 2018). The third group, represented principally by wood density (WD), stands in for plant hydraulics: denser wood tends to have lower permeability to water (Sperry, 2003; Lin et al., 2015). Wood density also directly influences plant growth because volume growth is necessarily slower, for a given photosynthetic output, in trees with dense wood. Relatively more carbon also needs to be allocated to high-density wood, at the

234 expense of allocation to leaves and fine roots. Although the correlation between WD
235 and more directly instrumental traits for plant hydraulics, such as the Huber value (the
236 ratio of cross-sectional sapwood area to subtended leaf area) (Togashi et al., 2015),
237 vessel density and calibre, and permeability (Reid et al., 2005) is imperfect, these last
238 traits are much more time-consuming to measure than WD and thus comparatively
239 under-represented in available data sets. We anticipate that plants with a lavish water
240 use strategy should present high conductivity and low-density wood, while plants
241 adapted to environments with long droughts, or vulnerable to water use competition,
242 should tend to adopt a conservative water-use strategy and to have high-density wood.
243 The fourth group reflects the ability to compete with other species for light, expressed
244 as potential maximum height (H_{max}): taller plants are able to harvest more light while
245 shorter plants are often more shade-tolerant (Turner, 2001). This group includes χ,
246 which has been reported to show a negative relationship with tree height (Koch et al.,
247 2015). The reason χ belongs with H_{max} and not with V_{cmax} in this analysis is because
248 we have intentionally restricted the climatic range to moist forests, so that the
249 variation in χ is mainly related to plant strategy rather than to aridity or temperature.
250 H_{max} is considered to be a species characteristic and although it may not be reached at
251 every site, its use as an indicator of plant strategy is likely better than using actual
252 observed height, which varies among individuals and over time.
253 Leaf-level measurements were conducted in tropical forests of Queensland,
254 Australia and Yunnan, China, and combined with (a) published and unpublished
255 datasets on H_{max}, WD, and (b) expert knowledge of the species' vegetation dynamical
256 roles (climax, subcanopy, large and small pioneers). Thus we are able to present what
257 is (to our knowledge) the first study to analyse key biochemical rates in the context of
258 tree species' contrasting dynamic roles, and the first empirical trait-based analysis to
259 include measured biochemical rates in a PFT classification with the aim to inform
260 progress in DGVM development. The objective of this work was to quantify trait
261 variation within these forests that can be linked to dynamical roles, but also
262 specifically to test the following predictions: (i) when moisture supply and low
263 temperatures are not limiting factors, photosynthetic capacity should be governed by
264 incident PAR (a prediction of the coordination hypothesis); (ii) χ should be lower at
265 high H_{max} (a prediction of the least-cost hypothesis); and (iii) pioneer species should

tend to have low WD, an expectation from the theory of forest dynamics (Shugart, 1984).

Materials and methods

Study Sites

Our analysis includes material from 232 evergreen angiosperm tree species (431 leaf samples) from moist tropical forests of Queensland, northern Australia (Robson Creek on the inland Atherton Tablelands to Cape Tribulation near the Pacific coast) and Yunnan, southwestern China (the Xishuangbanna region in southern Yunnan, near the land borders with Myanmar, Thailand and Laos). Field campaigns conducted in Queensland and Yunnan yielded data on 191 species. Data from these campaigns were combined with data on a further 41 Queensland species from field studies carried out by the TROpical Biomes In Transition (TROBIT) network (Bloomfield et al., 2014). Climates covered by the sampled areas range in mean annual precipitation (MAP) from 1427 to 5143 mm (Liddell, 2013b, a; Harris et al., 2014; Hutchinson, 2014c) and in mean annual temperature (MAT) between 19.0 and 24.4 ˚C (Liddell, 2013b, a; Harris et al., 2014; Hutchinson, 2014a, b). Both Queensland and Yunnan have a marked wet season and 'dry' (drier) season, and although the range of MAP values is considerable, all the sites correspond to climates where moisture is unlikely to be a limiting factor for forest development. The drier season at the Queensland and Yunnan sites lasts four to five months, but there is still typically 100-300 mm precipitation per month. Gridded climatological data at 0.01˚ resolution for 1971-2000 on MAP, MAT, annual Moisture Index (MI, the ratio of precipitation to equilibrium evaporation) and mean monthly photosynthetic active radiation (mPAR) were acquired for the Australian sites at www.tern.org.au. Climatological data for the Chinese sites were derived from records at 1814 meteorological stations (740 stations have observations from 1971-2000, the rest from 1981-1990: China Meteorological Administration, unpublished data), interpolated to a 0.01˚ grid using a three dimensional thin-plate spline (ANUSPLIN version 4.36, Hancock and Hutchinson, 2006). Fig. 1 and Table 1 provide further details on sites and climates.

Gas exchange measurements and photosynthetic variables

We used a portable infrared gas analyser (IRGA) system (LI-6400; Li-Cor, Inc., Lincoln, NB, USA) to perform leaf gas-exchange measurements. Sunlit terminal branches from the top one-third of the canopy were collected and immediately re-cut under water. One of the youngest fully expanded leaves, attached to the branch, was sealed in the leaf chamber. Measurements in the field were taken with relative humidity and chamber block temperature close to those of the ambient air at the time of measurement. The rate of airflow was held constant at 500 μmol s^{-1}, but exceptionally the flow was reduced (to a minimum of 250 μmol s^{-1}) under very low stomatal conductance.

We obtained 130 *A*-c_i curves from 41 species from Robson Creek (*RCR1* and *RCR2*) in both the dry and the wet season. The CO_2 mixing ratios for the *A*-c_i curves proceeded stepwise down from 400 to 35 and up to 2000 μmol mol^{-1}. Prior to the measurements, we tested plants to determine appropriate light-saturation levels. The photosynthetic photon flux density (PPFD) adopted for measurement ranged between 1500 and 1800 μmol m^{-2} s^{-1}. After measuring the *A*-c_i curves over about 35 minutes, light was set to zero for five minutes before measuring respiration. This was a time-saving compromise to allow four or five replicate curves per machine per day, based on our experience that stable results are commonly obtained after five minutes. Moreover, this quick estimate should be superior to the common practice of deriving R_{dark} as one of the parameters in a curve-fitting routine. Following the protocol of Domingues et al. (2010), we discarded 37 of a total 167 *A*-c_i curves in which stomatal conductance (g_s) declined to very low levels, adversely affecting the calculation of V_{cmax}. These procedures were very similar to the ones applied to the 125 *A*-c_i curves obtained from 26 species in the TROBIT sites (*CTR2*, *KBL1*, *KBL3* and *KCR*) during the wet season, further described in Bloomfield et al. (2014).

We sampled 114 leaves of 91 species in Yunnan (*Y1X*, *Y2U*, *Y3M1*, *Y3M2*, *Y4L*) in the dry season. Data for 62 leaves of 16 species were also obtained from Cape Tribulation in the dry season *(CTR1:*Weerasinghe et al., 2014). We used the same sampling methods for Yunnan and for Cape Tribulation. PPFD was held constant at 1800 μmol m^{-2} s^{-1}. For each leaf, we first set the CO_2 mixing ratio to 400 μmol mol^{-1} to obtain the rate of photosynthesis under light saturation (A_{sat}). Measurement was taken under stable g_s (> 0.5 μmol m^{-2} s^{-1}), CO_2 and leaf-to-air vapour pressure deficit.

The next step was to increase the CO_2 mixing ratio to 2000 μmol mol^{-1} in order to register the rate of photosynthesis under light and CO_2 saturation (A_{max}). R_{dark} was not measured in Yunnan. For R_{dark} in *CTR1*, the leaf was wrapped in foil sheets after A_{sat} and A_{max} measurements. There was a waiting period of at least 30 minutes of darkness before taking R_{dark} values.

Values of V_{cmax} and J_{max} were fitted using the Farquhar et al. (1980) model. The assumption of unlimited mesophyll conductance (Miyazawa and Kikuzawa, 2006; Lin et al., 2013) remains the standard implementation of the Farquhar model although it is recognized to be an approximation that results in an overestimation of V_{cmax} and J_{max}. Hence all of the values estimated are 'apparent' V_{cmax} and J_{max} values, as in most of the ecophysiological literature. In cases where A-c_i curves were not measured, we estimated V_{cmax} from A_{sat} by the so-called one-point method, which inverts the equation for Rubisco-limited photosynthesis taking into account the measured c_i and leaf temperature by applying the temperature dependencies of the Michaelis-Menten coefficients of Rubisco for carboxykation (K_C) and oxygenation (K_O) and the photorespiratory compensation point (Γ^*) from Bernacchi et al. (2001). The one-point method relies on the assumption that light-saturated photosynthesis measured on field-grown plants is Rubisco-limited, which has been found to be true in almost all cases (De Kauwe et al., 2016). J_{max} was estimated from A_{max} on the assumption that high CO_2 forces the leaves into electron-transport limitation (Bernacchi et al., 2003). Triose phosphate utilization limitation was not considered, as it would be unlikely to occur at our field temperatures > 22 ˚C (Sharkey et al., 2007; Lombardozzi et al., 2018)

Nutrient analyses

After completion of the leaf gas-exchange measurements, the leaf was retained to determine leaf area, dry mass, and mass-based N and P concentrations (N_{mass} and P_{mass}, mg g^{-1}). Leaves were sealed in plastic bags containing moist tissue paper to prevent wilting. Leaf area was determined using a 600 dot/inch flatbed top-illuminated optical scanner and Image J software (http://imagej.nih.gov/ij/). Leaves were dried in a portable desiccator for 48 hours for preservation until the end of the campaign and subsequently oven-dried in the laboratory for 24 hours at 70˚C. Then the dry weight was determined (Mettler-Toledo Ltd, Port Melbourne, Victoria,

Australia). LMA (g m^{-2}) was calculated from leaf area and dry mass. N_{mass} and P_{mass} were obtained by Kjeldahl acid digestion of the same leaves (Allen et al., 1974). The leaf material was digested using 98% sulphuric acid and 30% hydrogen peroxide. Digested material was analyzed for *N* and *P* using a flow injection analyser system (LaChat QuikChem 8500 Series 2, Lachat Instruments, Milwaukee, WI, USA). N_{area} and P_{area} (mg m^{-2}) were calculated as products of LMA and N_{mass} or P_{mass}. TROBIT nutrient analysis was performed using similar methods but different equipment, as described in Bloomfield et al. (2014).

Wood density and tree height

Twenty-year series of wood density (*WD*), tree height (*H*), and tree diameter at breast height (*D*) were obtained from Bradford et al. (2014a) (n = 138). Maximum tree height (H_{max}) was estimated using the derivative of the Mitscherlich function relating diameter and height (Li et al., 2014):

$$dH/dD = a \exp(-aD/H_{max}) = a(1 - H/H_{max}) \quad (1)$$

where *a* is the initial slope of the relationship between height and diameter. A typical range of *a* in the literature is 116 ± 4.35.

Dynamic roles of species

Australian species (n = 61) were assigned to dynamic roles with the help of the database published by Bradford et al. (2014b) and expert knowledge by MB. Chinese species (n = 85) were assigned to dynamic roles based on expert knowledge by ZH. These 'expert' classifications (A1) were compared with a quantitative trait-based classification (A2) as described in the next section. Both classification approaches were implemented according to the Shugart (1984) framework, which can also be related to those of Denslow (1987), Turner (2001) and Fyllas et al. (2012):

(1) Requires a gap, and produces a gap. These are long-lived pioneers that reach the canopy. Shade intolerant.

(2) Does not require a gap, but produces a gap. These are long-lived climax species that reach the canopy and grow large. Shade tolerant.

(3) Requires a gap, but does not produce a gap. These are short-lived pioneers that never grow large. Shade intolerant.
(4) Does not require a gap, and does not produce a gap. These are sub-canopy species. Shade tolerant.

The geographic distribution of expert assessment of dynamic roles per number of species and per number of leaves is shown in Table 2. This dataset includes 262 observations.

Statistical analyses

All statistics were performed in `R` (R Core Team, 2012). For graphing we used the `ggplot2` package (Wickham, 2010). Moisture index was represented in Fig. 1 as its square root, a transformation appropriate to precipitation values (M.F. Hutchinson, personal communication, 2011), which approximately normalizes the distribution of values and thus contains the large spread of values at the high end. V_{cmax}, J_{max}, R_{dark}, LMA, N_{area}, P_{area}, H_{max} and WD data were $\log_{10}$-transformed, unless otherwise indicated, achieving an approximately normal distribution of values. χ was logit-transformed as this variable is bounded between 0 and 1, and the logit transformation results in approximately linear relationships between the transformed ratio and environmental predictors, including temperature (Wang et al., 2017). Ordinary least-squares linear regression was used to test relationships between plant traits and climate variables. Pairwise combinations of quantitative traits were tested for significant relationships across all data, and within groups corresponding to high and low MI, high and low mPAR, and high and low MAT. Slopes and elevations of regressions were compared using standardized major axis regression with the `smatr` package (Warton et al., 2006). The package `vegan` (Oksanen et al., 2015) was used to assess multivariate trait variation, using the following methods:

- Principal component analysis (PCA) of nine plant traits (V_{cmax}, J_{max}, R_{dark}, LMA, N_{area}, P_{area}, H_{max}, WD and χ);
- Redundancy analysis (RDA) of the same nine traits, constrained by three climate variables (MI, mPAR and MAT);
- RDA of the same nine traits, constrained by dynamic roles (as factors); and

- RDA of the same nine traits constrained simultaneously by both climate and dynamic roles.

PCA was used to identify patterns of covariation among traits irrespective of their dynamic or environmental correlates, and RDA to analyse multivariate trait relationships to predictors. Note that PCA is an exploratory method with no associated formal test of significance. By contrast, the significance of trait-environment relationships identified by RDA can be assessed approximately in a similar way to generalized linear models (Ter Braak and Prentice, 1988). The *K*-means (R Core Team, 2012) clustering method was used to create four groups of species based on the nine plant traits (A2: Dynamic roles based on quantitative assessment). *K*-means clustering was performed with the number of iterations set to 100 and bootstrapped with 10,000 repetitions. RDA and bivariate correlations were used to compare classifications A2 and A1. The dataset used for PCA and RDA analysis consisted of 130 observations with information for all traits, climate variables and dynamic roles. All RDA visualizations here follow the response-variable focused 'Type 2 scaling' (Oksanen et al., 2015), such that the angles between pairs of vectors as plotted approximate their pairwise correlations. For PCA and RDA input data where direct measurements of R_{dark} were not available, R_{dark} (n = 58) was estimated from A_{sat} following Prentice et al. (2014) using the approximation $R_{dark} \approx 0.01\ V_{cmax}$ (De Kauwe et al., 2016).

Research data

Robson Creek (*RCR1* and *RCR2*) data can be requested at www.tern.org.au (Prentice et al., 2013). Access to TROBIT data (*CTR2*, *KBL1*, *KBL3* and *KCR*) and Cape Tribulation 1 (*CTR1*) are described in Bloomfield et al. (2014) and Weerasinghe et al. (2014) respectively. For Yunnan data (*Y1X*, *Y2U*, *Y3M1*, *Y3M2*, *Y4L*), refer to Wang et al. (2018).

Results

Trait values and dimensions of variation

Average values of the metabolic traits V_{cmax}, J_{max}, and R_{dark} were 52.0, 82.0, and 0.63 μmol m^{-2} s^{-1} respectively. The corresponding ranges were 4.2 to 148.9, 14.0

to 203.6, and near zero to 3.70 μmol m^{-2} s^{-1}. Average values of the chemical/structural traits LMA, N_{area} and P_{area} were 110.9 × 10^3, 0.19 × 10^3 and 0.013 g m^{-2} with ranges of 12.04 to 610.3 × 10^3 (LMA), near zero to 1.49 g m^{-2} (N_{area}), and near zero to 0.06 mg m^{-2} (P_{area}). Average values of χ, H_{max} and WD were 0.71, 26.3 m and 0.55 g cm^{-3} with ranges of 0.39 to 0.94, 1.3 to 54.5 m, and 0.33 to 0.98 g cm^{-3} respectively.

Four orthogonal dimensions of trait variation were identified corresponding to the metabolic, chemical/structural, hydraulic and height trait groups described above (Fig. 2, Table 3). The metabolic traits V_{cmax}, J_{max} and R_{dark} varied continuously and in close correlation with one another. V_{cmax} and χ were negatively correlated, but the correlation was weak (not shown: slope = –1.85, intercept = 1.32, R^2 = 0.13, p < 0.05). Table 3 makes it clear that variation in χ in this data set does not belong to the metabolic dimension. The chemical/structural traits LMA, N_{area} and P_{area} were positively correlated with one another (p < 0.05), although the pairwise relationship of P_{area} to LMA was weaker than that of N_{area} to LMA. The strong correlation between LMA and N_{area} suggests that much of the N content in the leaves is structural rather than metabolic (see also Yang et al., 2018). A similar result was obtained when mass- rather than area-based nutrient values were used in the PCA (not shown). The third dimension was mostly represented by variation in WD, with some contribution from P_{area}. Finally H_{max} and χ had a non-significant negative pairwise relationship and were associated with the fourth dimension, suggesting a trade-off between water loss and the length of the water-transport pathway. These dimensions of trait variation are broadly in agreement with those described by Baraloto et al. (2010), Fyllas et al. (2012) and Reich (2014).

Contribution of climate variables to trait variation

High and low values for MI, mPAR and MAT were defined as values above or below the mean value of the climate variable. Regression slopes between V_{cmax} and J_{max} for both high MI and low MI groups were close together but statistically distinct (p < 0.05, Fig. 3), and the same was true for high *versus* low mPAR and MAT groups (Fig. 3). Regressions for V_{cmax} *versus* N_{area} were not significant within these climatic groups (Fig. 3) but the relationship was significant, albeit weak, when all of the data were considered together (not shown: slope = 0.69, R^2 = 0.10, p < 0.05). The

484 weakness of this relationship corroborates our previous assessment of leaf N content
485 as being primarily structural rather than metabolic. High MI and low mPAR were
486 associated with high V_{cmax}, J_{max}, and N_{area} (Fig. 3). These variables were also
487 associated with R_{dark} and LMA. The remaining traits χ, P_{area}, H_{max} and WD were very
488 scattered against MI and mPAR (no significant relationship). All traits had high and
489 low values spanning the full range of MAT.
490 The clustered vectors for metabolic traits, MI and MAT in Fig. 4 indicate that
491 higher moisture and air temperature favour species with higher metabolic rates (Fig.
492 4). The RDA constrained by climate variables explained 35% of trait variation with
493 19% and 11% on axes 1 and 2 respectively ($p < 0.05$, Fig. 4). This represents an
494 unexpectedly large fraction of the trait variation, considering the modest range in
495 MAT (19 to 24˚C), mPAR (27.4 to 30.5 mol m^{-2}) and MI (0.9 to 2.5; i.e. typical
496 values for non-drought-stressed conditions) among these tropical moist forest sites.
497 No individually significant trait-climate variable relationship was found. An
498 association of high metabolic rates with aridity (Prentice et al., 2011) has been found
499 when considering longer climate gradients, but this is not apparent over the more
500 limited climatic range sampled here.

501 **Contribution of dynamic roles to trait variation**

502 The assignment of the four groups obtained by *K*-means clustering to dynamic
503 roles was based on the degree of correspondence between the mean values of plant
504 traits for each group and the classification by Shugart (1984). H_{max} determined
505 whether a cluster was labeled as climax or large pioneer, or small pioneer or
506 subcanopy. Higher values of photosynthetic traits defined tall trees as climax, as
507 opposed to large pioneer, and small trees as small pioneer, as opposed to subcanopy.
508 Expert (A1) and quantitative (A2) role definitions explained 23% and 55% of
509 total plant trait variance, respectively (Fig. 5). With respect to patterns, the RDA
510 results obtained with the two classifications are quite similar to one another, which is
511 expected as the clustering was performed using the same trait data represented in the
512 RDA. However, the quantitative role definitions explained substantially more
513 variance than the expert definitions. The major common patterns shown in the two
514 RDA plots are as follows:
515

(1) The metabolic traits V_{cmax}, J_{max}, R_{dark} and the structural-chemical traits N_{area} and LMA tend to be higher in climax species than in the other groups.
(2) P_{area} tends to be greater in subcanopy species than in the other groups.
(3) WD tends to be smaller in pioneer species than in the other groups.

These distinctions are supported, and further information provided, by the summary statistics for trait variation within each group (Fig. 6). Climax species consistently have the highest values of V_{cmax}, J_{max}, R_{dark}, LMA and N_{area}. High WD, consistent with slow growth, characterized the subcanopy species. The χ ratio was lowest in climax species and highest in subcanopy species. The scaling slopes of the bivariate relationships between V_{cmax} and J_{max}, and between V_{cmax} and $N_{area,}$ were largely similar within each group, whether the roles were defined quantitatively or by expert assessment (Fig. 7).

Partitioning trait variance to climate variables *versus* dynamic roles

RDA constrained by the two sets of predictors (climate and dynamic roles) both separately and collectively provides the necessary information to partition the total explained variation into the unique contributions of each set and a combined contribution associated with covariation of the two sets, via the Legendre variation partitioning method (Legendre and Anderson, 1999; Peres-Neto et al., 2006; Meng et al., 2015; Yang et al., 2018). Based on the quantitative assessment of dynamic roles (A2), RDA constrained by both sets of predictors explained 61% of trait variation, which could be partitioned as follows: 26% from dynamic roles alone, 6% from climate alone, and 29% from the combination. The corresponding figures based on expert assessment were as follows: 43% of trait variation explained, composed of 8% from dynamic roles alone, 20% from climate alone, and 15% from the combination.

Although significant trait variation was linked to climate, individual trait-climate relationships were weak and patterns that have been observed across a wider range of climates, such as the widely reported increase of N_{area} with aridity, were not present. This pattern is to be expected considering that semi-arid and arid ecosystems are not considered. Variance partitioning showed that between 8 and 26% of trait variation (depending on the source of information on dynamics roles) could not be

attributed to the temperature and moisture regime, but could be related uniquely to species' dynamic roles.

Unexplained trait variance

Unexplained variance amounted to 57% and 39% for the expert and quantitative assessments, respectively. In principle unexplained variance might be related to a variety of factors including the season of measurement, forest age and aspects of soil fertility. However, dividing the data according to wet-season (*CTR2*, *KBL1*, *KBL3*, *KCR*, *RCRs*) *versus* dry-season (*CTR1*, *RCRw*, *Y1X*, *Y2U*, *Y3M1*, *Y3M2*, *Y4L*) measurements yielded patterns similar to those found in the full data set. No data on forest age were available. No correlations were found between trait values and soil total N, soil total P and cation exchange capacity (Table 1).

Discussion

This study provides support for the idea that forest dynamic roles, as described by Shugart (1984), might be systematically related to the biophysical and ecophysiological traits used in DGVMs. Our analysis explores plant trait diversity and plasticity with a view to more realistic modelling of plant and vegetation processes, whether for local or global model applications (Fyllas et al., 2009; 2012; Quesada et al., 2012). Expert classification of dynamic roles in forests is notoriously difficult because it requires observation over many decades. Our quantitative analyses suggest a possible alternative approach to classification based on trait measurements at one point in time. Moreover, our results have supported certain specific predictions of the least-cost and coordination hypotheses, which are key to explaining species strategies, community assembly and ecosystem structure and function (Reich, 2014). They collectively hold the promise of providing general, testable trait-environment relationships that could reduce the excessive number of parameters required by most DGVMs (Prentice et al., 2015).

Dynamic roles and the coordination hypothesis

Our results support a core prediction of the coordination hypothesis for forests: that J_{max} and V_{cmax} should be higher under high illumination and lower in the

shade, as seen both in the vertical gradient of light-saturated assimilation rates in dense canopies (Chen et al., 1993) and more generally, in the solar radiation gradient across canopies situated in diverse environments (Maire et al., 2012). With respect to dynamic roles, outer-canopy climax species are expected to receive most PAR and therefore should have the highest photosynthetic capacity, while subcanopy species should have the lowest. Pioneer (gap-requiring) species would be expected to have intermediate photosynthetic capacity and this too is consistent with our findings. Additionally, the widely reported conservative ratio of J_{max} and V_{cmax} seems to be maintained, both within and across dynamic roles. The association of R_{dark} with V_{cmax} and J_{max} was also found to be strong, with R_{dark} maintaining a near constant ratio for leaves whether in sun-exposed or shade conditions, as previously reported (e.g. by Hirose and Werger, 1987; Weerasinghe et al., 2014; Atkin et al., 2015).

The observed relationships among N_{area}, P_{area} and LMA, and the weaker correlations of these traits with primary metabolic traits, reflect the fact that a substantial part of the N and P content of leaves is not directly tied to photosynthetic functions (Dong et al., 2017). Although strong linear relationships between V_{cmax} (at a reference temperature) and N_{area} seem to be widely expected, they are not always found (Prentice et al., 2014; Togashi et al., 2017), perhaps due to the overpowering effect of variation in structural and/or defensive components of leaf N. The photosynthetic component of N_{area} however is expected to be proportional to incident PAR. This expectation is supported by the analysis of Dong et al. (2017), and by our finding of highest N_{area} among climax species.

Dynamic roles and the least-cost hypothesis

It has been reported that χ declines with tree height. This too is a prediction of the least-cost hypothesis (Prentice et al., 2014), as the cost of maintaining the water transport pathway increases at with height. Therefore, tall trees – and the top stratum of leaves in a tall tree, as noted by Koch et al. (2015) – may be expected to aim for a lower optimum χ by investing more in the maintenance of biochemical capacity and less in the maintenance of transport capacity. Even if the path-length effect on stem hydraulic conductance is fully compensated by xylem tapering (Tyree and Ewers, 1991; Enquist and Bentley, 2012; Olson et al., 2014) as often seems to be the case, it is still more expensive in terms of sapwood respiration to maintain a tall stem as

opposed to a short stem (Prentice et al., 2014). This prediction is supported by the low χ found here in climax species. However, surprisingly, large pioneer species (with H_{max} equivalent to climax species) did not show this adaptation. Subcanopy species did nonetheless show high χ, consistent with their short stature. Given a reduced χ, the coordination hypothesis then predicts that V_{cmax} should be increased. This mechanism may additionally contribute to the high V_{cmax} found in climax species and the low V_{cmax} in subcanopy species.

Dynamic roles, the leaf economics spectrum and the theory of forest dynamics

A third group of predictions broadly supported by our results comes from the framework presented in Shugart (1984), Turner (2001) and Fyllas et al. (2012). This approach considers two main axes of ecological specialization, one reflecting canopy position and access to light, the other life span and growth rate. The main advantage for large pioneers in rapidly achieving tall stature is to shade lower canopies nearby, while obtaining rapid access to full sunlight. Compared to climax species, large pioneers adopt a less conservative strategy regarding water use, and are likely to have a shorter lifespan (Shugart, 1984; Reich, 2014). One way to achieve fast growth is to invest in low-density conducting tissues, which implies lower WD. Subcanopy species by contrast are necessarily shade-tolerant and often have traits associated with slow growth. Our results support the existence of this tradeoff, with subcanopy trees having generally high WD (a trait often accompanied by a high density of short and narrow vessels: Reich, 2014).

According to the LES, across species globally, high LMA is linked to longevity of individual leaves; and it has generally been found that LMA varies as much or more within communities as with environmental gradients (Wright et al., 2004). Our data do not allow us to address the LMA-lifespan linkage directly. However, they do show that LMA varies systematically across the dynamic roles, being greatest in climax species and associated with high V_{cmax} and least in subcanopy species where it is associated with low V_{cmax}. These findings suggest a more nuanced interpretation of the variation in LMA among dynamic roles. Namely: that thick, high-LMA leaves are a pre-requisite for a leaf to attain V_{cmax} commensurate with high levels of PAR at the top of a canopy (Niinemets and Tenhunen, 1997), while thin, low-LMA leaves provide optimum light capture for the least investment in leaves – a

641 good strategy for subcanopy species. Fast-growing pioneer species with their high
642 water-use strategy also require a low investment in leaf structure, developing thin,
643 low-LMA leaves in order to obtain a quicker return on investment (Turner, 2001).
644 The downside is that these leaves are likely to be more exposed to herbivory losses,
645 while the low-density stems are subject to the risks of cavitation and embolism,
646 shortening their life expectancy (Enquist and Bentley, 2012).

647 **Implications for modelling**

648 DGVMs based on continuous trait variation have been developed in response
649 to the growing realization that PFTs, as conventionally defined, do not adequately
650 describe the genotypic or phenotypic plasticity of plant traits in the real world. The
651 existence of systematic, adaptive trait variation in forests, within a climate range
652 where neither moisture nor low temperature is limiting, provides further support for
653 the conclusion (e.g. Meng et al., 2015) that models should not be based on fixed,
654 PFT-specific values for many quantitative traits. In general, consideration of the
655 adaptive function of trait differences among dynamic roles should contribute to
656 reducing the multiplicity of uncertain parameters, and simultaneously increase the
657 realism, of next-generation DGVMs. DGVMs in general (including recent trait-based
658 vegetation models, with the exception of the model of Fyllas et al., 2014 developed
659 for Amazonian forests) have paid minimal attention to the co-existing functional
660 diversity of traits present in communities where climate variation is small but tree
661 species diversity is large, including tropical forests. Our results suggest that the
662 framework provided by optimality concepts (the coordination and least-cost
663 hypotheses) could be combined with classical forest dynamics theory, which
664 differentiates complementary survival strategies for tree species in a highly
665 competitive environment, to yield successful predictions that would allow vegetation
666 dynamics to be represented more faithfully in DGVMs. The combination of these
667 different research strands can be achieved by extending existing predictions about
668 trait-environment relationships based on optimality considerations to cover biotically
669 induced microhabitat variation within complex plant communities.
670 We therefore suggest that the ecophysiological correlates of species dynamical
671 roles be further analysed in other tropical and extratropical forests, as part of the
672 empirical research required to establish a firmer foundation for next-generation

673 vegetation models. Moreover, we look forward to the widespread use of adaptive
674 schemes in which trait combinations, such as those characterizing species' dynamical
675 roles, emerge naturally from the competition among plants.
676
677 **Acknowledgments**

678 This research was funded by the Terrestrial Ecosystem Research Network
679 (TERN, www.tern.org.au), which has been supported by the Australian Government
680 through the National Collaborative Research Infrastructure Strategy (NCRIS), with
681 additional funding provided by Macquarie University and the Australian National
682 University. HFT and ND were supported by Macquarie University International
683 Research Scholarship (iMQRES) awards to ICP. ICP, BJE, HFT and ND have been
684 supported by the Ecosystem Modelling and Scaling Infrastructure Facility (eMAST,
685 http://www.emast.org.au). Data were collected in North Queensland at field sites of
686 the Australian SuperSite Network. Both eMAST and the Australian SuperSites
687 Network are facilities of TERN. OA acknowledges the support of the Australian
688 Research Council (DP130101252 and CE140100008). Leaf N and P mesaurements
689 were made at the Department of Forestry, ANU. We are grateful to Jinlong Zhang
690 (Xishuangbanna Tropical Botanical Garden) for identifying plant species, and also to
691 Jack Egerton (ANU), Li Guangqi (Macquarie), Lingling Zhu (ANU), Danielle Creek
692 (University of Western Sydney), Lucy Hayes (ANU) and Stephanie McCaffery
693 (ANU) for help with fieldwork and/or N and P digestions. We thank Tomas Ferreira
694 Domingues (University of São Paulo) for comments that helped to improve this paper.
695 ND and SPH acknowledge support from the ERC-funded project GC2.0 (Global
696 Change 2.0: Unlocking the past for a clearer future, grant number 694481). This
697 research is a contribution to the AXA Chair Program in Biosphere and Climate
698 Impacts and the Imperial College initiative on Grand Challenges in Ecosystems and
699 the Environment (ICP).

Tables

Table 1. Climate averages (MAT = mean annual temperature, MI = Moisture Index, mPAR = mean monthly photosynthetic active radiation), geographic location, elevation above sea level and soil properties (CEC = cation exchange capacity, TN = total soil nitrogen, TP = total soil phosphorus) of the study sites in north-east Australia (*CTR1*, *CTR2*, *KBL1*, *KBL3*, *KCR*, *RCRs*, *RCRw*) and south-east China (*Y1X*, *Y2U*, *Y3M1*, *Y3M2*, *Y4L*).

SITE	LON	LAT	Altitude (m)	MAT (°C)	MAP (mm)	mPAR (mol/m^2)	MI	CEC(cmol/kg)	TN (%)	TP (%)
CTR1	145.45	-16.10	64	24.4	5143	27.5	2.54	11.8	0.64	0.023
CTR2	145.45	-16.10	90	24.4	5143	27.5	2.54	11.8	0.02	0.011
KBL1	145.54	-17.76	761	20.4	1976	28.2	1.39	10.83	0.08	0.030
KBL3	145.54	-17.69	1055	19.0	1726	28.3	1.22	11.11	0.08	0.030
KCR	145.60	-17.11	813	19.6	2541	27.9	1.82	9.81	0.01	0.006
RCRs	145.63	-17.12	700	19.4	2246	27.9	1.29	4.3	0.18	0.019
RCRw	145.63	-17.12	700	19.4	2246	27.9	1.29	4.3	0.18	0.019
Y1X	101.27	21.92	502	21.7	1427	30.1	0.94	8.68	0.08	0.044
Y2U	101.24	21.98	1075	19.7	1562	30.6	1.03	6.09	0.08	0.044
Y3M1	101.58	21.61	668	19.6	1662	29.8	1.14	10.21	0.08	0.050
Y3M2	101.58	21.62	828	20.5	1604	29.9	1.07	10.21	0.08	0.050
Y4L	101.58	21.62	1034	20.5	1604	30.1	1.06	10.21	0.08	0.050

Table 2. Geographic distribution of expert assessment of dynamic roles per number of species and per number of leaves for the study sites in north-east Australia (*CTR1*, *CTR2*, *KBL1*, *KBL3*, *KCR*, *RCRs*, *RCRw*) and south-east China (*Y1X*, *Y2U*, *Y3M1*, *Y3M2*, *Y4L*). This dataset includes 262 observations.

SITE	Number of species				Number of leaves			
	climax	large pioneer	Small pioneer	subcanopy	climax	large pioneer	Small pioneer	subcanopy
CTR1	7	4		1	27	16		4
CTR2	4	1			11	5		
KBL1	2	4			7	25		
KBL3	3	4			17	13		
KCR	3	5			9	17		
RCRs	7	16	3	4	9	52	7	4
RCRw		8	1			26	4	
Y1X		2				2		
Y2U		3		1		3		1
Y3M1				1				2
Y3M2				1				1
Y4L								

Table 3. Principal Component Analysis loadings for nine traits. The highest correlations (absolute magnitudes > 0.45) are indicated in bold.

	PC1	PC2	PC3	PC4
log V_{cmax}	**-0.48**	-0.27	0.21	0
log J_{max}	**-0.46**	-0.25	0.18	0.04
log R_{dark}	**-0.45**	-0.16	0.27	-0.01
log LMA	-0.32	**0.55**	-0.21	0.03
log N_{area}	-0.37	**0.45**	-0.24	-0.12
log P_{area}	-0.08	**0.54**	**0.45**	0.03
log WD	0.15	0.1	**0.68**	-0.16
log H_{max}	-0.2	-0.15	-0.24	**-0.74**
logit χ	0.23	0.11	0.16	**-0.64**
	PC1	PC2	PC3	PC4
Standard deviation	1.84	1.26	1.09	0.98
Proportion of Variance	0.37	0.18	0.13	0.11
Cumulative Proportion	0.37	0.55	0.68	0.79

716 **Figures**

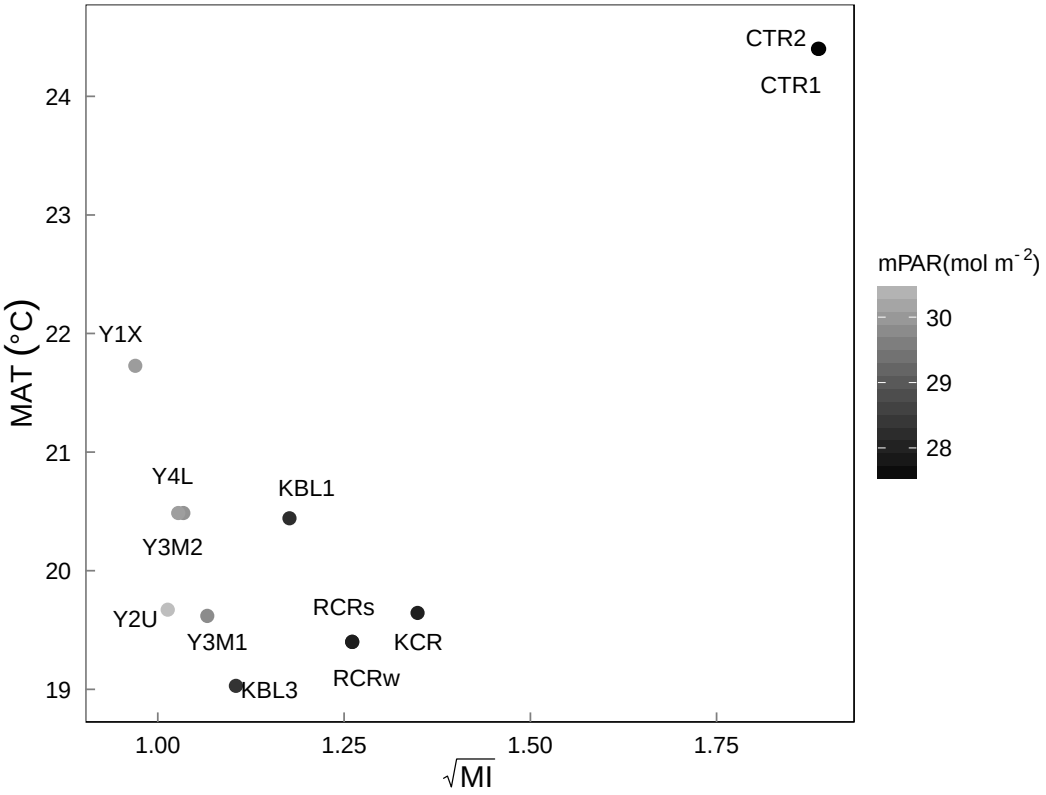

717

718 Fig. 1. Mean annual temperature (MAT, ^{o}C), the square root of Moisture Index (MI,
719 ratio of precipitation to equilibrium evapotranspiration) and mean monthly
720 photosynthetic active radiation (mPAR, mol m^{-2}) for northern Australia (*CTR1*,
721 *CTR2*, *KBL1*, *KBL3*, *KCR*, *RCRs*, *RCRw*) and southwestern China (*Y1X*, *Y2U*, *Y3M1*,
722 *Y3M2*, *Y4L*).

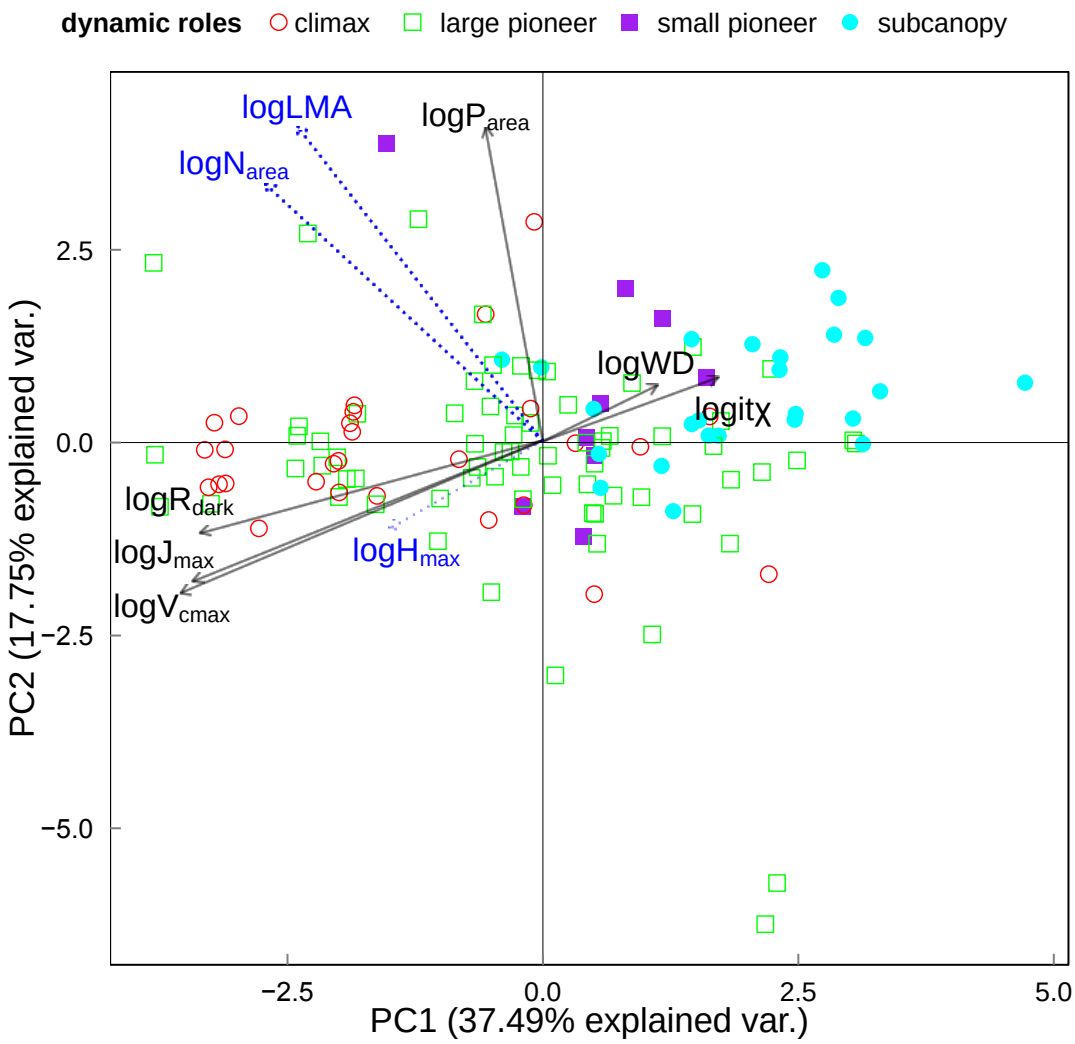

723

724 Fig. 2. Principal component analysis (PCA) of nine traits in northern Australia and
725 southwestern China (*n* = 130). Blue dotted lines and names extend backwards from
726 the plane of the paper; and black lines and names protrude forwards towards the
727 observer.

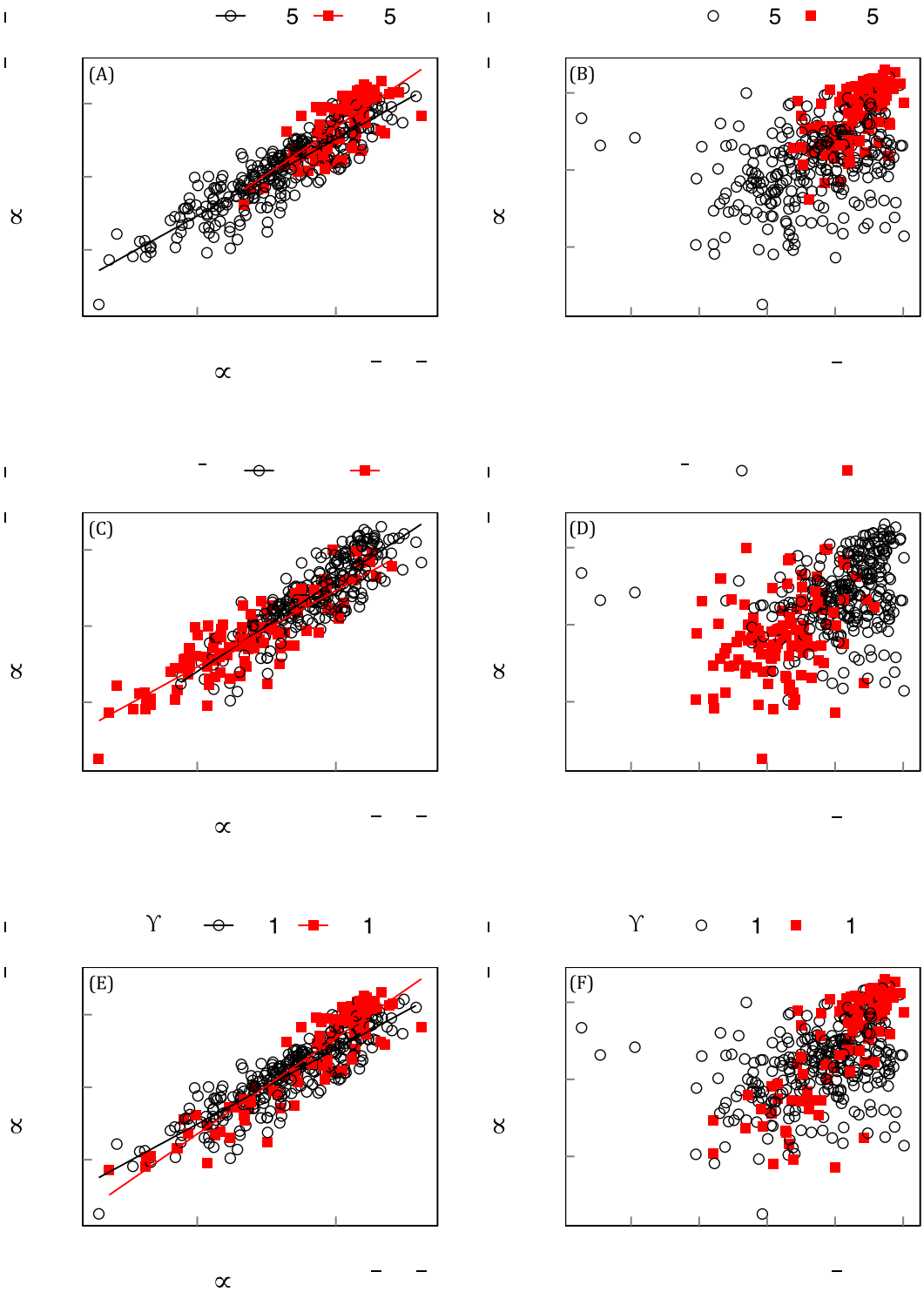

Fig. 3. Bivariate relationships of $\log_{10}V_{cmax}$ *versus* $\log_{10}J_{max}$ and $\log_{10}V_{cmax}$ *versus* $\log_{10}N_{area}$, within groups defined by high and low values of climate variables (3A and 3B: MI; 3C and 3D: mPAR; 3E and 3F: MAT) (n = 431). Only significant linear regressions ($p < 0.05$) are shown.

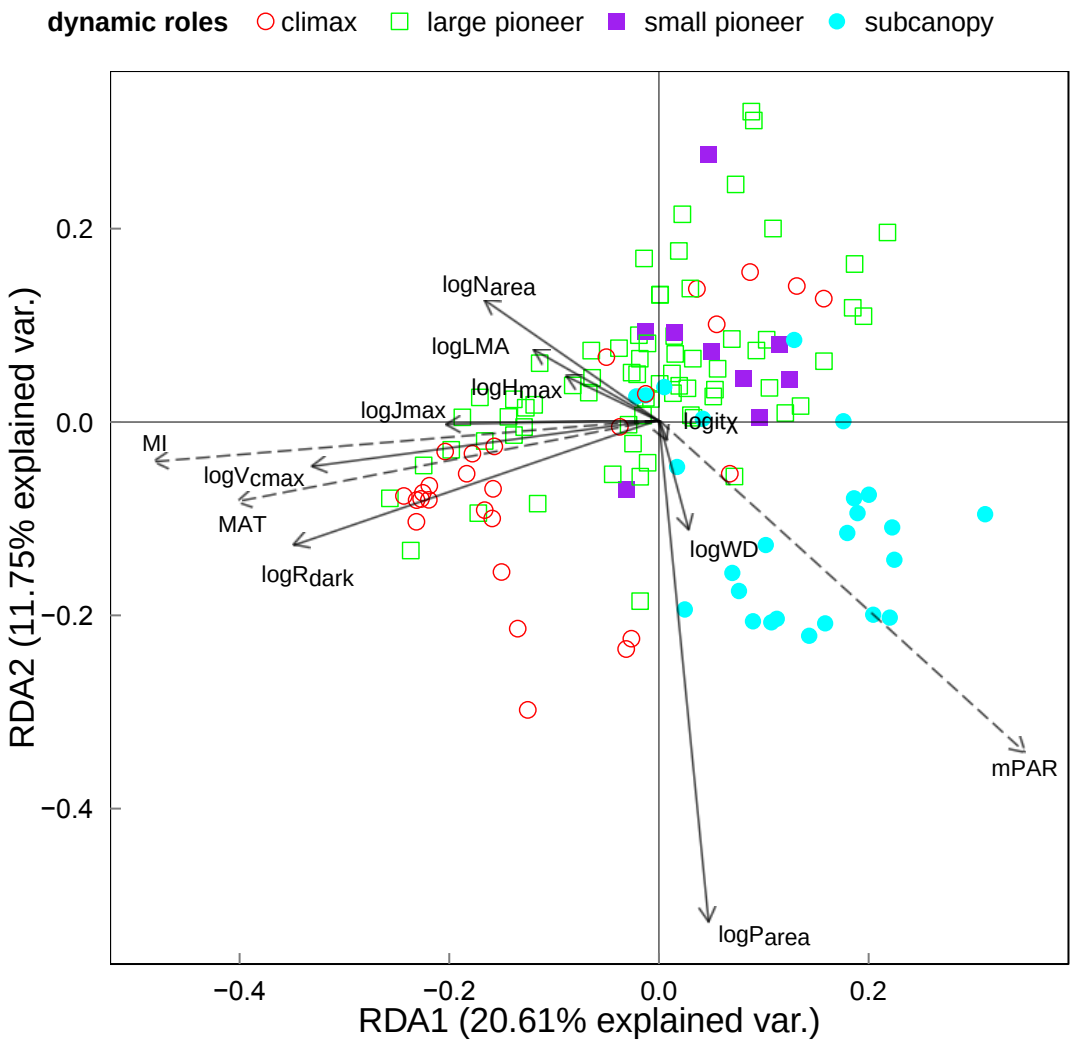

Fig. 4. Redundancy analysis (RDA) of nine traits constrained by climate variables Mean annual temperature (MAT, ^{o}C), the square root of Moisture Index (MI, ratio of precipitation to equilibrium evapotranspiration) and mean monthly photosynthetic active radiation (mPAR, mol m^{-2}) (n = 130, $p < 0.05$). Dynamic roles do not participate in this RDA calculation and are shown for visual comparison only.

742

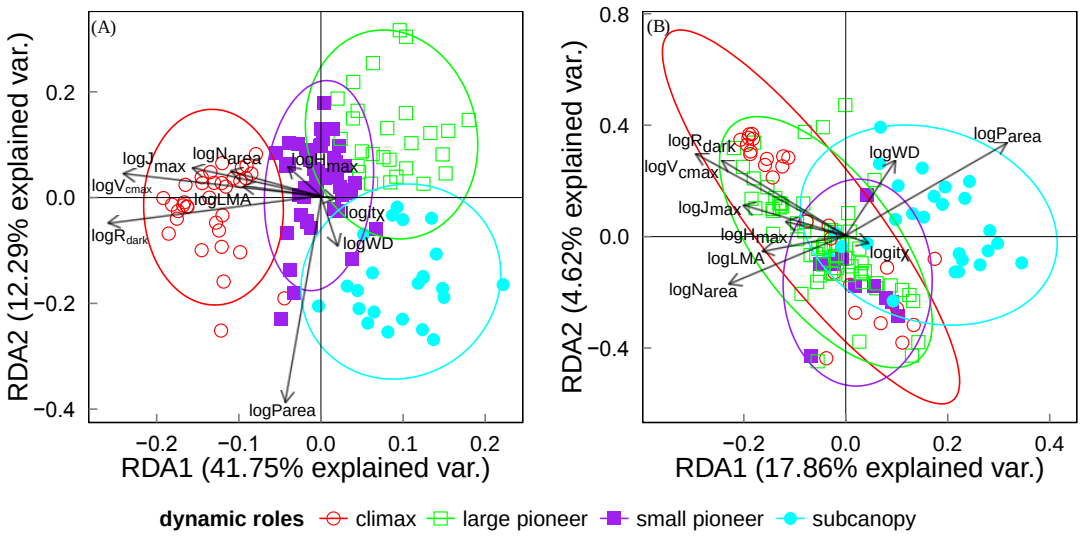

743

744 Fig. 5. Redundancy analysis (RDA) of nine traits constrained by dynamic roles,

745 defined by quantitative (5A) *versus* expert (5B) assessment (n = 130). Ellipses

746 represent 95% confidence intervals around the centroid of each group.

747

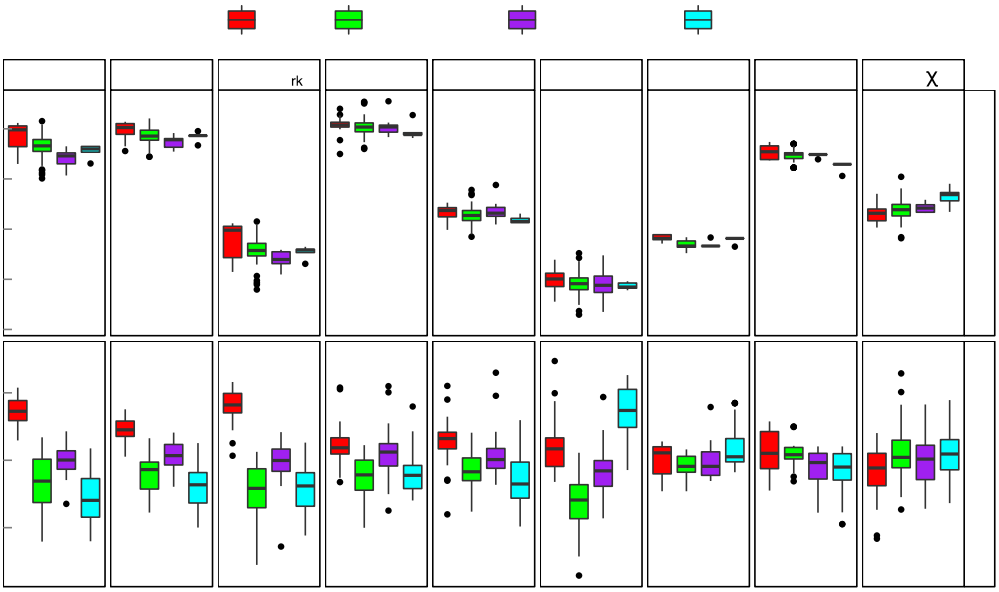

Fig. 6. Box plots showing means and standard deviation of nine traits according to the four dynamic roles based on quantitative *versus* expert assessment (n = 130, p < 0.05). 'Expert' group averages of LMA, N_{area} land P_{area} are not significantly different (ANOVA). Dynamic roles of each trait sharing the same letter (Tukey *post hoc* test) are not significantly different.

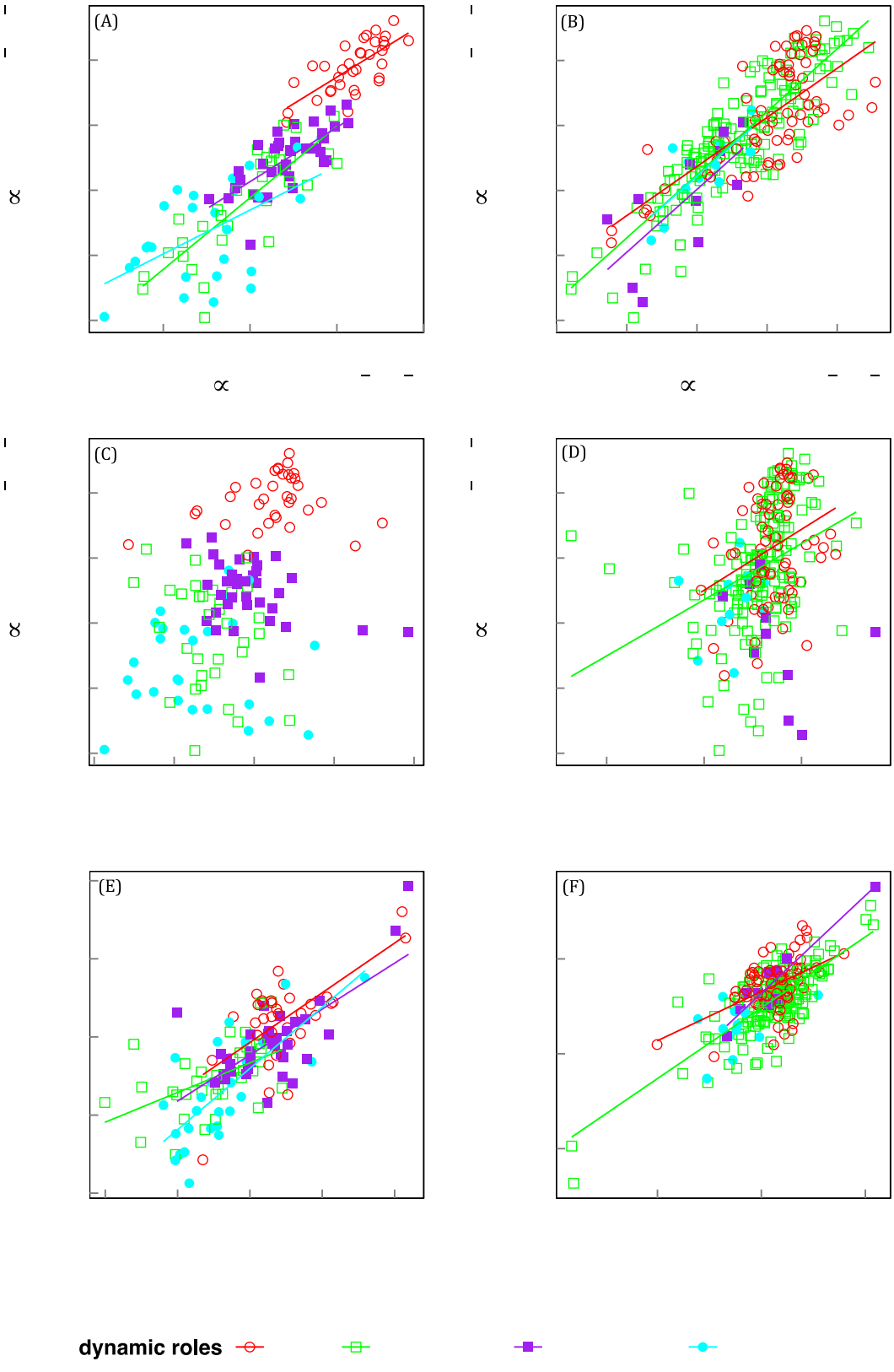

755

756 Fig. 7. Bivariate relationships of V_{cmax} *versus* J_{max}, V_{cmax} *versus* N_{area} (upper panels)

757 and N_{area} *versus* LMA (lower panels) within dynamic role groups, according to

quantitative (left, $n = 130$) *versus* expert (right, $n = 262$) assessment. Significant linear regressions between $\log_{10}$-transformed variables are shown ($p < 0.05$).

References

Allen, S.E., Grimshaw, H., Parkinson, J.A., Quarmby, C., 1974. Chemical analysis of ecological materials. Blackwell Scientific Publications.

Atkin, O.K., Bloomfield, K.J., Reich, P.B., Tjoelker, M.G., Asner, G.P., Bonal, D., Bönisch, G., Bradford, M.G., Cernusak, L.A., Cosio, E.G., Creek, D., Crous, K.Y., Domingues, T.F., Dukes, J.S., Egerton, J.J.G., Evans, J.R., Farquhar, G.D., Fyllas, N.M., Gauthier, P.P.G., Gloor, E., Gimeno, T.E., Griffin, K.L., Guerrieri, R., Heskel, M.A., Huntingford, C., Ishida, F.Y., Kattge, J., Lambers, H., Liddell, M.J., Lloyd, J., Lusk, C.H., Martin, R.E., Maksimov, A.P., Maximov, T.C., Malhi, Y., Medlyn, B.E., Meir, P., Mercado, L.M., Mirotchnick, N., Ng, D., Niinemets, Ü., O'Sullivan, O.S., Phillips, O.L., Poorter, L., Poot, P., Prentice, I.C., Salinas, N., Rowland, L.M., Ryan, M.G., Sitch, S., Slot, M., Smith, N.G., Turnbull, M.H., VanderWel, M.C., Valladares, F., Veneklaas, E.J., Weerasinghe, L.K., Wirth, C., Wright, I.J., Wythers, K.R., Xiang, J., Xiang, S., Zaragoza-Castells, J., 2015. Global variability in leaf respiration in relation to climate, plant functional types and leaf traits. New Phytologist 206, 614–636.

Atkin, O.K., Holly, C., Ball, M.C., 2000. Acclimation of snow gum (*Eucalyptus pauciflora*) leaf respiration to seasonal and diurnal variations in temperature: the importance of changes in the capacity and temperature sensitivity of respiration. Plant, Cell & Environment 23, 15-26.

Baraloto, C., Timothy Paine, C., Poorter, L., Beauchene, J., Bonal, D., Domenach, A.M., Hérault, B., Patino, S., Roggy, J.C., Chave, J., 2010. Decoupled leaf and stem economics in rain forest trees. Ecology Letters 13, 1338-1347.

Bernacchi, C.J., Pimentel, C., Long, S.P., 2003. In vivo temperature response functions of parameters required to model RuBP-limited photosynthesis. Plant, Cell & Environment 26, 1419-1430.

Bernacchi, C.J., Singsaas, E.L., Pimentel, C., Portis Jr, A.R., Long, S.P., 2001. Improved temperature response functions for models of Rubisco-limited photosynthesis. Plant, Cell & Environment 24, 253-259.

Bloomfield, K.J., Domingues, T.F., Saiz, G., Bird, M.I., Crayn, D.M., Ford, A., Metcalfe, D.J., Farquhar, G.D., Lloyd, J., 2014. Contrasting photosynthetic characteristics of forest vs. savanna species (far North Queensland, Australia). Biogeosciences 11, 7331-7347, https://doi.org/7310.5194/bg-7311-7331-2014.

Botkin, D.B., Janak, J.F., Wallis, J.R., 1972. Some ecological consequences of a computer model of forest growth. The Journal of Ecology, 849-872.

Box, E.O., 1981. Predicting physiognomic vegetation types with climate variables. Vegetatio 45, 127-139.

Bradford, M.G., Metcalfe, D.J., Ford, A., Liddell, M.J., McKeown, A., 2014a. Floristics, stand structure and aboveground biomass of a 25-ha rainforest plot in the wet tropics of Australia. Journal of Tropical Forest Science 26, 543-553.

Bradford, M.G., Murphy, H.T., Ford, A.J., Hogan, D.L., Metcalfe, D.J., 2014b. Long-term stem inventory data from tropical rain forest plots in Australia. Ecology 95, 2362-2000.

Calvin, M., Benson, A.A., 1948. The path of carbon in photosynthesis. US Atomic Energy Commission, Technical Information Division.

Chen, J.-L., Reynolds, J., Harley, P., Tenhunen, J., 1993. Coordination theory of leaf nitrogen distribution in a canopy. Oecologia 93, 63-69.

De Kauwe, M.G., Lin, Y.-S., Wright, I.J., Medlyn, B.E., Crous, K.Y., Ellsworth, D.S., Maire, V., Prentice, I.C., Atkin, O.K., Rogers, A., Niinemets, Ü., Serbin, S.P., Meir, P., Uddling, J., Togashi, H.F., Tarvainen, L., Weerasinghe, L.K., Evans, B.J., Ishida, F.Y.,

Domingues, T.F., 2016. A test of the 'one-point method' for estimating maximum carboxylation capacity from field-measured, light-saturated photosynthesis. New Phytologist 210, 1130-1144.
Denslow, J.S., 1987. Tropical rainforest gaps and tree species diversity. Annual Review of Ecology and Systematics 18, 431-451.
Dewar, R., Mauranen, A., Mäkelä, A., Hölttä, T., Medlyn, B., Vesala, T., 2018. New insights into the covariation of stomatal, mesophyll and hydraulic conductances from optimization models incorporating nonstomatal limitations to photosynthesis. New Phytologist 217, 571-585.
Díaz, S., Cabido, M., 1997. Plant functional types and ecosystem function in relation to global change. Journal of Vegetation Science 8, 463-474.
Domingues, T.F., Meir, P., Feldpausch, T.R., Saiz, G., Veenendaal, E.M., Schrodt, F., Bird, M., Djagbletey, G., Hien, F., Compaore, H., Diallo, A., Grace, J., Lloyd, J.O.N., 2010. Co-limitation of photosynthetic capacity by nitrogen and phosphorus in West Africa woodlands. Plant, Cell & Environment 33, 959-980.
Dong, N., Prentice, I.C., Evans, B.J., Caddy-Retalic, S., Lowe, A.J., Wright, I.J., 2017. Leaf nitrogen from first principles: field evidence for adaptive variation with climate. Biogeosciences 14, 481-495.
Enquist, B.J., Bentley, L.P., 2012. Land plants: new theoretical directions and empirical prospects. Metabolic Ecology: A Scaling Approach. Hoboken, NJ: Wiley-Blackwell, 164-187.
Evans, J., 1989. Photosynthesis and nitrogen relationships in leaves of C_3 plants. Oecologia 78, 9-19.
Farquhar, G.D., von Caemmerer, S., Berry, J.A., 1980. A biochemical model of photosynthetic CO2 assimilation in leaves of C3 species. Planta 149, 78-90.
Fisher, R., Muszala, S., Verteinstein, M., Lawrence, P., Xu, C., McDowell, N., Knox, R., Koven, C., Holm, J., Rogers, B., 2015. Taking off the training wheels: the properties of a dynamic vegetation model without climate envelopes, CLM4.5(ED) Geoscientific Model Development 8, 3593–3619.
Friend, A., Schugart, H., Running, S., 1993. A physiology-based gap model of forest dynamics. Ecology 74, 792-797.
Fyllas, N., Gloor, E., Mercado, L., Sitch, S., Quesada, C., Domingues, T., Galbraith, D., Torre-Lezama, A., Vilanova, E., Ramírez-Angulo, H., 2014. Analysing Amazonian forest productivity using a new individual and trait-based model (TFS v. 1). Geoscientific Model Development 7, 1251-1269.
Fyllas, N.M., Patino, S., Baker, T., Bielefeld Nardoto, G., Martinelli, L., Quesada, C., Paiva, R., Schwarz, M., Horna, V., Mercado, L., 2009. Basin-wide variations in foliar properties of Amazonian forest: phylogeny, soils and climate. Biogeosciences 6, 2677-2708.
Fyllas, N.M., Quesada, C.A., Lloyd, J., 2012. Deriving Plant Functional Types for Amazonian forests for use in vegetation dynamics models. Perspectives in Plant Ecology, Evolution and Systematics 14, 97-110.
Hancock, P., Hutchinson, M., 2006. Spatial interpolation of large climate data sets using bivariate thin plate smoothing splines. Environmental Modelling & Software 21, 1684-1694.
Harris, I., Jones, P.D., Osborn, T.J., Lister, D.H., 2014. Updated high-resolution grids of monthly climatic observations – the CRU TS3.10 Dataset. International Journal of Climatology 34, 623-642.

858 Harrison, S.P., Prentice, I.C., Barboni, D., Kohfeld, K.E., Ni, J., Sutra, J.P., 2010.
859 Ecophysiological and bioclimatic foundations for a global plant functional
860 classification. Journal of Vegetation Science 21, 300-317.
861 Haxeltine, A., Prentice, I.C., 1996. A General Model for the Light-Use Efficiency of
862 Primary Production. Functional Ecology 10, 551-561.
863 Hirose, T., Werger, M.J., 1987. Nitrogen use efficiency in instantaneous and daily
864 photosynthesis of leaves in the canopy of a Solidago altissima stand. Physiologia
865 Plantarum 70, 215-222.
866 Hutchinson, M., 2014a. Daily maximum precipitation: ANUClimate 1.0, 0.01
867 degree, Australian Coverage, 1970-2012.
868 Hutchinson, M., 2014b. Daily minimum temperature: ANUClimate 1.0, 0.01
869 degree, Australian Coverage, 1970-2012.
870 Hutchinson, M., 2014c. Daily precipitation: ANUClimate 1.0, 0.01 degree,
871 Australian Coverage, 1970-2012.
872 Koch, G.W., Sillett, S.C., Antoine, M.E., Williams, C.B., 2015. Growth maximization
873 trumps maintenance of leaf conductance in the tallest angiosperm. Oecologia
874 177, 321-331.
875 Köppen, W.P., 1931. Grundriss der klimakunde. Walter de Gruyter Berlin.
876 Kortschak, H.P., Hartt, C.E., Burr, G.O., 1965. Carbon dioxide fixation in sugarcane
877 leaves. Plant Physiology 40, 209.
878 Langan, L. , Higgins, S. I. and Scheiter, S., 2017. Climate ‐ biomes, pedo ‐ biomes
879 or pyro ‐ biomes: which world view explains the tropical forest – savanna
880 boundary in South America? Journal of Biogeography, 44: 2319-2330.
881 Lavorel, S., Garnier, E., 2002. Predicting changes in community composition and
882 ecosystem functioning from plant traits: revisiting the Holy Grail. Functional
883 Ecology 16, 545-556.
884 Legendre, P., Anderson, M.J., 1999. Distance ‐ based redundancy analysis: testing
885 multispecies responses in multifactorial ecological experiments. Ecological
886 Monographs 69, 1-24.
887 Li, G., Harrison, S.P., Prentice, I.C., Falster, D., 2014. Simulation of tree-ring widths
888 with a model for primary production, carbon allocation, and growth.
889 Biogeosciences 11, 6711-6724.
890 Liddell, M., 2013a. Cape Tribulation OzFlux tower site OzFlux: Australian and
891 New Zealand Flux Research and Monitoring TERN hdl: 102.100.100/14242.
892 Liddell, M., 2013b. Robson Creek OzFlux tower site OzFlux: Australian and New
893 Zealand Flux Research and Monitoring. TERN hdl: 102.100.100/14243.
894 Lin, Y.-S., Medlyn, B.E., De Kauwe, M.G., Ellsworth, D.S., 2013. Biochemical
895 photosynthetic responses to temperature: how do interspecific differences
896 compare with seasonal shifts? Tree Physiology 33, 793-806.
897 Lin, Y.-S., Medlyn, B.E., Duursma, R.A., Prentice, I.C., Wang, H., Baig, S., Eamus, D.,
898 de Dios, V.R., Mitchell, P., Ellsworth, D.S., de Beeck, M.O., Wallin, G., Uddling, J.,
899 Tarvainen, L., Linderson, M.-L., Cernusak, L.A., Nippert, J.B., Ocheltree, T.W.,
900 Tissue, D.T., Martin-StPaul, N.K., Rogers, A., Warren, J.M., De Angelis, P., Hikosaka,
901 K., Han, Q., Onoda, Y., Gimeno, T.E., Barton, C.V.M., Bennie, J., Bonal, D., Bosc, A.,
902 Low, M., Macinins-Ng, C., Rey, A., Rowland, L., Setterfield, S.A., Tausz-Posch, S.,
903 Zaragoza-Castells, J., Broadmeadow, M.S.J., Drake, J.E., Freeman, M., Ghannoum,
904 O., Hutley, L.B., Kelly, J.W., Kikuzawa, K., Kolari, P., Koyama, K., Limousin, J.-M.,
905 Meir, P., Lola da Costa, A.C., Mikkelsen, T.N., Salinas, N., Sun, W., Wingate, L., 2015.

Optimal stomatal behaviour around the world. Nature Climate Change 5, 459-464.
Lloyd, J., Bloomfield, K., Domingues, T.F., Farquhar, G.D., 2013. Photosynthetically relevant foliar traits correlating better on a mass vs an area basis: of ecophysiological relevance or just a case of mathematical imperatives and statistical quicksand? New Phytologist 199, 311-321.
Lombardozzi, D.L., Smith, N.G., Cheng, S.J., Dukes, J.S., Sharkey, T.D., Rogers, A., Fisher, R. and Bonan, G.B., 2018. Triose phosphate limitation in photosynthesis models reduces leaf photosynthesis and global terrestrial carbon storage. Environmental Research Letters 13(7), 074025.
Maire, V., Martre, P., Kattge, J., Gastal, F., Esser, G., Fontaine, S., Soussana, J.-F., 2012. The coordination of leaf photosynthesis links C and N fluxes in C_3 plant species. PLoS ONE 7, e38345.
Medlyn, B.E., Duursma, R.A., Eamus, D., Ellsworth, D.S., Prentice, I.C., Barton, C.V.M., Crous, K.Y., De Angelis, P., Freeman, M., Wingate, L., 2011. Reconciling the optimal and empirical approaches to modelling stomatal conductance. Global Change Biology 17, 2134-2144.
Medvigy, D., Wofsy, S.C., Munger, J.W., Hollinger, D.Y., Moorcroft, P.R., 2009. Mechanistic scaling of ecosystem function and dynamics in space and time: Ecosystem Demography model version 2. Journal of Geophysical Research: Biogeosciences 114, 0148-0227.
Meng, T., Wang, H., Harrison, S., Prentice, I., Ni, J., Wang, G., 2015. Responses of leaf traits to climatic gradients: adaptive variation versus competitional shifts. Biogeosciences 12, 5339-5352.
Miyazawa, Y., Kikuzawa, K., 2006. Physiological basis of seasonal trend in leaf photosynthesis of five evergreen broad-leaved species in a temperate deciduous forest. Tree Physiology 26, 249-256.
Moorcroft, P.R., Hurtt, G.C., Pacala, S.W., 2001. A method for scaling vegetation dynamics: The Ecosystem Demography Model (ED). Ecological Monographs 71, 557-586.
Niinemets, Ü., Tenhunen, J.D., 1997. A model separating leaf structural and physiological effects on carbon gain along light gradients for the shade-tolerant species Acer saccharum. Plant, Cell & Environment 20, 845-866.
Oksanen, J., Blanchet, F.G., Kindt, R., Legendre, P., Minchin, P.R., O'Hara, R., Simpson, G.L., Solymos, P., Stevens, M.H.H., Wagner, H., 2015. Package 'vegan'. Community ecology package, version, 2.2-1.
Olson, M.E., Anfodillo, T., Rosell, J.A., Petit, G., Crivellaro, A., Isnard, S., León‐Gómez, C., Alvarado‐Cárdenas, L.O., Castorena, M., 2014. Universal hydraulics of the flowering plants: vessel diameter scales with stem length across angiosperm lineages, habits and climates. Ecology Letters 17, 988-997.
Pavlick, R., Drewry, D.T., Bohn, K., Reu, B., Kleidon, A., 2013. The Jena Diversity-Dynamic Global Vegetation Model (JeDi-DGVM): a diverse approach to representing terrestrial biogeography and biogeochemistry based on plant functional trade-offs. Biogeosciences 10, 4137-4177.
Peres-Neto, P.R., Legendre, P., Dray, S., Borcard, D., 2006. Variation partitioning of species data matrices: estimation and comparison of fractions. Ecology 87, 2614-2625.
Prentice, I., Leemans, R., 1990. Pattern and process and the dynamics of forest structure: a simulation approach. The Journal of Ecology, 340-355.

955 Prentice, I.C., Bondeau, A., Cramer, W., Harrison, S.P., Hickler, T., Lucht, W., Sitch,
956 S., Smith, B., Sykes, M.T., 2007. Dynamic global vegetation modeling: quantifying
957 terrestrial ecosystem responses to large-scale environmental change, Terrestrial
958 ecosystems in a changing world. In: Canadell J.G., Pataki D.E., Pitelka L.F. (eds)
959 Terrestrial Ecosystems in a Changing World. Global Change — The IGBP Series.
960 Springer, Berlin, Heidelberg, pp. 175-192.
961 Prentice, I.C., Cowling, S.A., 2013. Dynamic global vegetation models, in: Levin,
962 S.A., Academic Press (Ed.), Encyclopedia of Biodiversity, 2nd edition ed, pp. 607-
963 689.
964 Prentice, I.C., Cramer, W., Harrison, S.P., Leemans, R., Monserud, R.A., Solomon,
965 A.M., 1992. A global biome model based on plant physiology and dominance, soil
966 properties and climate. Journal of Biogeography 19, 117-134.
967 Prentice, I.C., Dong, N., Gleason, S.M., Maire, V., Wright, I.J., 2014. Balancing the
968 costs of carbon gain and water transport: testing a new theoretical framework
969 for plant functional ecology. Ecology Letters 17, 82-91.
970 Prentice, I.C., Liang, X., Medlyn, B.E., Wang, Y.P., 2015. Reliable, robust and
971 realistic: the three R's of next-generation land-surface modelling. Atmospheric
972 Chemistry and Physics 15, 5987-6005.
973 Prentice, I.C., Liddell, M., Furstenau Togashi, H., Atkin, O., Weerasinghe, L., 2013.
974 Leaf Level Physiology, Chemistry and Structural Traits, Far North Queensland
975 SuperSite, Robson Creek, 2012. TERN Australian SuperSite Network.
976 http://portal.tern.org.au/leaf-level-physiology-creek-2012 12.
977 Prentice, I.C., Meng, T., Wang, H., Harrison, S.P., Ni, J., Wang, G., 2011. Evidence of
978 a universal scaling relationship for leaf CO_2 drawdown along an aridity gradient.
979 New Phytologist 190, 169-180.
980 Prentice, I.C., Sykes, M.T., Cramer, W., 1993. A simulation model for the transient
981 effects of climate change on forest landscapes. Ecological Modelling 65, 51-70.
982 Purves, D.W., Lichstein, J.W., Strigul, N., Pacala, S.W., 2008. Predicting and
983 understanding forest dynamics using a simple tractable model. Proceedings of
984 the National Academy of Sciences 105, 17018.
985 Quesada, C.A., Phillips, O.L., Schwarz, M., Czimczik, C.I., Baker, T.R., Patino, S.,
986 Fyllas, N.M., Hodnett, M.G., Herrera, R., Almeida, S., Alvarez Dávila, E., Arneth, A.,
987 Arroyo, L., Chao, K. J., Dezzeo, N., Erwin, T., di Fiore, A., Higuchi, N., Honorio
988 Coronado, E., Jimenez, E. M., Killeen, T., Lezama, A. T., Lloyd, G., López-González,
989 G., Luizão, F. J., Malhi, Y., Monteagudo, A., Neill, D. A., Núñez Vargas, P., Paiva, R.,
990 Peacock, J., Peñuela, M. C., Peña Cruz, A., Pitman, N., Priante Filho, N., Prieto, A.,
991 Ramírez, H., Rudas, A., Salomão, R., Santos, A. J. B., Schmerler, J., Silva, N., Silveira,
992 M., Vásquez, R., Vieira, I., Terborgh, J., and Lloyd, J., 2012. Basin-wide variations
993 in Amazon forest structure and function are mediated by both soils and climate.
994 Biogeosciences 9, 2203-2246.
995 R Core Team, 2012. R: A language and environment for statistical computing. R
996 Foundation for Statistical Computing, Vienna, Austria. http://www.R-
997 project.org/.
998 Ranson, S.L., Thomas, M., 1960. Crassulacean Acid Metabolism. Annual Review of
999 Plant Physiology 11, 81-110.
1000 Raunkiær, C., 1934. The Life Forms of Plants and Statistical Plant Geography.
1001 Clarendon Press.
1002 Reich, P.B., 2014. The world-wide 'fast–slow' plant economics spectrum: a traits
1003 manifesto. Journal of Ecology 102, 275-301.

Reich, P.B., Walters, M.B., Ellsworth, D.S., 1997. From tropics to tundra: global convergence in plant functioning. Proceedings of the National Academy of Sciences 94, 13730-13734.
Reid, D.E.B., Silins, U., Mendoza, C., Lieffers, V.J., 2005. A unified nomenclature for quantification and description of water conducting properties of sapwood xylem based on Darcy's law. Tree Physiology 25, 993-1000.
Sakschewski, B., Bloh, W., Boit, A., Rammig, A., Kattge, J., Poorter, L., Peñuelas, J., Thonicke, K., 2015. Leaf and stem economics spectra drive diversity of functional plant traits in a dynamic global vegetation model. Global Change Biology 21, 2711-2725.
Scheiter, S., Langan, L., Higgins, S.I., 2013. Next ‐ generation dynamic global vegetation models: learning from community ecology. New Phytologist 198, 957-969.
Sharkey, T.D., Bernacchi, C.J., Farquhar, G.D., Singsaas, E.L., 2007. Fitting photosynthetic carbon dioxide response curves for C_3 leaves. Plant, Cell & Environment 30, 1035-1040.
Shugart, H.H., 1984. A Theory of Forest Dynamics. Springer-Verlag, New York.
Sitch, S., Smith, B., Prentice, I.C., Arneth, A., Bondeau, A., Cramer, W., Kaplan, J.O., Levis, S., Lucht, W., Sykes, M.T., Thonicke, K., Venevsky, S., 2003. Evaluation of ecosystem dynamics, plant geography and terrestrial carbon cycling in the LPJ dynamic global vegetation model. Global Change Biology 9, 161-185.
Smith, B., Prentice, I.C., Sykes, M.T., 2001. Representation of vegetation dynamics in the modelling of terrestrial ecosystems: comparing two contrasting approaches within European climate space. Global Ecology and Biogeography 10, 621-637.
Sperry, John S., 2003. Evolution of water transport and xylem structure. International Journal of Plant Sciences 164, S115-S127.
Swaine, M., Whitmore, T., 1988. On the definition of ecological species groups in tropical rain forests. Vegetatio 75, 81-86.
Ter Braak, C.J., Prentice, I.C., 1988. A theory of gradient analysis. Advances in Ecological Research 18, 271-317.
Togashi, H.F., Prentice, I.C., Atkin, O.K., Macfarlane, C., Prober, S., Bloomfield, K.J., Evans, B., 2017. Thermal acclimation of leaf photosynthetic traits in an evergreen woodland, consistent with the co-ordination hypothesis. Biogeosciences Discuss., https://doi.org/10.5194/bg-2017-449, in review, 2017.
Togashi, H.F., Prentice, I.C., Evans, B.J., Forrester, D.I., Drake, P., Feikema, P., Brooksbank, K., Eamus, D., Taylor, D., 2015. Morphological and moisture availability controls of the leaf area-to-sapwood area ratio: analysis of measurements on Australian trees. Ecology and Evolution 5, 1263-1270.
Turner, I.M., 2001. The Ecology of Trees in the Tropical Rain Forest. Cambridge University Press.
Tyree, M.T., Ewers, F.W., 1991. The hydraulic architecture of trees and other woody plants. New Phytologist 119, 345-360.
van Bodegom, P.M., Douma, J.C., Verheijen, L.M., 2014. A fully traits-based approach to modeling global vegetation distribution. Proceedings of the National Academy of Sciences 111, 13733.
Verheijen, L., Brovkin, V., Aerts, R., Bönish, G., Cornelissen, J., Kattge, J., Reich, P., Wright, I., Van Bodegom, P., 2013. Impacts of trait variation through observed

trait-climate relationships o performance of a representative Earth System Model: a conceptual analysis. Biogeosciences 10, 5497-5515.
Wang, H., Harrison, S.P., Prentice, I.C., Yang, Y., Bai, F., Togashi, H.F., Wang, M., Zhou, S., Ni, J., 2018. The China Plant Trait Database: toward a comprehensive regional compilation of functional traits for land plants. Ecology 99, 500-500.
Wang, H., Prentice, I.C., Keenan, T.F., Davis, T.W., Wright, I.J., Cornwell, W.K., Evans, B.J., Peng, C., 2017. Towards a universal model for carbon dioxide uptake by plants. Nature Plants 3, 734-741.
Warton, D.I., Wright, I.J., Falster, D.S., Westoby, M., 2006. Bivariate line‐fitting methods for allometry. Biological Reviews 81, 259-291.
Weerasinghe, L.K., Creek, D., Crous, K.Y., Xiang, S., Liddell, M.J., Turnbull, M.H., Atkin, O.K., 2014. Canopy position affects the relationships between leaf respiration and associated traits in a tropical rainforest in Far North Queensland. Tree Physiology 34, 564-584.
Whitehead, D., Edwards, W.R.N., Jarvis, P.G., 1984. Conducting sapwood area, foliage area, and permeability in mature trees of *Picea sitchensis* and *Pinus contorta*. Canadian Journal of Forest Research 14, 940-947.
Whitmore, T., 1982. On pattern and process in forests. In: Newman, E. I. (ed.), The plant community as a working mechanism. pp. 45–59. Blackwell, Oxford.
Wickham, H., 2010. ggplot2: Elegant Graphics for Data Analysis. Springer.
Woodward, F.I., 1987. Climate and Plant Distribution. Cambridge University Press.
Wright, I.J., Reich, P.B., Westoby, M., Ackerly, D.D., Baruch, Z., Bongers, F., Cavender-Bares, J., Chapin, T., Cornelissen, J.H.C., Diemer, M., Flexas, J., Garnier, E., Groom, P.K., Gulias, J., Hikosaka, K., Lamont, B.B., Lee, T., Lee, W., Lusk, C., Midgley, J.J., Navas, M.-L., Niinemets, U., Oleksyn, J., Osada, N., Poorter, H., Poot, P., Prior, L., Pyankov, V.I., Roumet, C., Thomas, S.C., Tjoelker, M.G., Veneklaas, E.J., Villar, R., 2004. The worldwide leaf economics spectrum. Nature 428, 821-827.
Yang, Y. , Wang, H. , Harrison, S.P., Prentice, I.C., Wright, I.J., Peng, C., Lin, G., 2018. Quantifying leaf - trait covariation and its controls across climates and biomes. New Phytologist (online). doi:10.1111/nph.15422
Zhou, S., Duursma, R.A., Medlyn, B.E., Kelly, J.W. and Prentice, I.C., 2013. How should we model plant responses to drought? An analysis of stomatal and non-stomatal responses to water stress. Agricultural and Forest Meteorology 182, 204-214.